JOURNAL OF APPLIED ELECTROCHEMISTRY 21 (1991) 805–815

Amino-alcohol electrosynthesis. Modelling of a set-up for producing amino-2-methyl-2-propanediol-1.3

A. SAVALL, J. QUESADO

Laboratoire de Génie Chimique et Electrochimie, URA CNRS 192, Université Paul Sabatier, 118 Route de Narbonne, 31062 Toulouse, France

M. RIGNON, J. MALAFOSSE

L'Air Liquide, Département Chimique, BP 111, Cité des Varennes, 71103 Chalon sur Saône, France

Received 20 December 1990; revised 14 March 1991

A nitro-alcohol electrochemical reduction process for the industrial production of amino-alcohols is described. The reaction takes place according to the scheme:

$$RNO_2 \longrightarrow RNHOH \longrightarrow RNH_2$$

The hydroxylamine forms on a copper cathode on which a zinc deposit forms during electrolysis and this catalyzes the formation of the amine. Electro-electrodialysis is used to separate the amino-alcohol obtained as a concentrated solution from the sulphuric acid. The electrolysis cell is coupled with a recycling tank and production is discontinuous. The model proposed integrates in the cathodic process: the consecutive electrochemical reactions described above, electrodeposition of zinc and evolution of hydrogen. The calculation takes into account the limitation of the reactions by the mass transfer together with the increase in volume of the catholyte during electrolysis. The model enables anticipation of the variation in the concentration of the various species with time and the duration of the electrolysis in the galvanostatic mode; it also enables assessment of thermal release due to irreversibilities. The influence of operating conditions such as initial reagent concentration, programming current density, ratio of the electrode surface with reagent quantity and electrolyte flow is presented. It is shown that for the operating conditions used in practice quasi-full conversion of the amino-alcohols may be achieved without reaching the stage where hydroxylamine is exhausted as characterized by the limitation through mass transfer.

Notation

A	electrode area (m^2)
b	width of the electrode (m)
C_i	concentration of species i ($mol\,m^{-3}$)
D_i	diffusion coefficient ($m^2\,s^{-1}$)
D_e	equivalent diameter of the cell $= 2bh/(b + h)$ (m)
F	Faraday's constant
h	distance between cathode and membrane (m)
I	current (A)
I_i	partial current for reaction i (A)
$i_{i,l}$	limiting current for reaction i (A)
i	current density ($A\,m^{-2}$)
$k(E)$	heterogeneous rate constant ($m\,s^{-1}$)
k_i	average mass transfer coefficient ($m\,s^{-1}$)
M_i	$= 1 - \exp(-k_i A/N)$
n_i	mole number of species i
$\dot{n}_i$	rate of reaction i ($mol\,m^{-2}\,s^{-1}$)
P_{elect}	electrical power supplied to the reactor ($kJ\,m^{-2}\,s^{-1}$)
P_{th}	heat power to be removed for isothermal operation ($kJ\,m^{-2}\,s^{-1}$)
N	volumic flow rate ($m^3\,s^{-1}$)
Q_t	total charge at time t (C)
$Q_{i,t}$	charge in relation with reaction i at time t (C)
R, R_t	accumulated current yield, instantaneous current yield
Re	Reynolds number $= vDe/v$
S	reduction stage (Equation 11)
Sc	Schmidt number $= v/D_i$
t	time (s)
t_{H2}	time after which hydrogen evolution reaction starts (s)
t_{ci}	critical time for reaction i (s)
U	cell voltage (V)
v	liquid velocity in the cathodic compartment ($m\,s^{-1}$)
V	catholyte volume (m^3)
$V_{m,i}$	molar volume of species i ($m^3\,mol^{-1}$)
z_i	electron number transferred in the electrode reaction i
ΔH_i	enthalpy of reaction i ($kJ\,mol^{-1}$)
$\Delta Q_{i,t}$	charge variation for reaction i (C)
Δt	time increment (s)
ΔV	catholyte volume variation for a Δt variation (m^3)
Δv	catholyte volume variation for 1 F (m^3)

0021-891X/91 $03.00 + .12

Greek symbols

ϕ	associating factor for the solvent in the Wilke and Chang correlation
θ	temperature (° C)
τ	residence time in the reservoir (s)
ν	kinematic viscosity ($m^2 s^{-1}$)
ω	rotating rate of the electrode ($rd s^{-1}$)
γ	specific constant for the rotating electrode hemisphere: $\gamma = 0.451 rd^{-1}(rd^{-1})$

Additional scripts

0	starting time
f	final time
t	time
i	reaction or product number
$i = 1$	NMPD or RNO_2
$i = 2$	HAMPD or RNHOH
$i = 3$	Zn^{2+}
$i = 4$	AMPD or RNH_2

1. Introduction

Amino-alcohols make up a family of products widely used in the manufacture of cosmetics and detergents, or as synthesis intermediates for antiseptics and pharmaceutical products. They are prepared through reduction of nitro-alcohols obtained by condensation of nitro-paraffins (CH_3NO_2, $C_2H_5NO_2$ . . .) with formaldehyde. The reduction of nitro-alcohols may be obtained by using the Fe/Fe^{2+} couple in a sulphuric or acetic acid medium. If this process is used, large quantities of solid residue must be eliminated. It is necessary to separate the amine by distillation; yield is in the order of 80% [1, 2]. In the case of catalytic hydrogenation, for example using Raney nickel in methanolic medium under 60 bar pressure between 40 and 45° C, yield does not exceed 80%. Furthermore, side reactions leading to the formation of shorter amines, heavy residues and N-methylated derivatives that are difficult to separate, make it not a very profitable method [1, 2].

Electrochemical processes, operating in favourable conditions, avoid the formation of side products. Although numerous studies of the reduction of nitro-derivatives by electrochemical means have been undertaken [3–5], few studies have led to industrial application where nitro-alcohols are concerned. However, a patent [6] describes a process in which the electrochemical reduction of nitro-alcohols is performed in a sulphuric or hydrochloric aqueous solution. The amine is separated once the ammonium salt solution has been neutralized.

L'AIR LIQUIDE recently improved [1, 2] a reduction process by electrochemical means in a sulphuric aqueous medium for obtaining a solution with a high concentration of pure amino-alcohol that is then separated from H_2SO_4 using electro-electrodialysis (EED). The nitro-alcohols are converted to their corresponding amines with yields of over 80%, and furthermore, the sulphuric acid solutions can be reused. Examples of the amino-alcohols envisaged include: tris-(hydroxymethyl)aminomethane, amino-2-methyl-2-propanediol-1.3, amino-2-propanediol-1.3, and amino-2-butanol-1.

This manufacturing process has been studied at pilot scale in filter-press type electrolysis cells, with an area of up to 1.6 m^2. In this type of installation the electrolysis reactor is associated with a recycling tank and production is discontinuous. Duration of electrolysis is a critical parameter when such installations are used. Consequently, a modelling study was developed with the aim of simulating the galvanostatic operation of the electrolysis device [7, 8]. The present study is concerned with electrosynthesis of amino-2-methyl-2-propanediol-1.3 (AMPD) using nitro-2-methyl-2-propanediol-1.3 (NMPD) as feedstock; however, the results can easily be extrapolated to the reduction of the other nitro-alcohols mentioned above or even to electrolysis of other less soluble nitrated derivatives. Operating conditions and results of the preparative electrolyses for these products are described in reference [2].

The amino-alcohol electrosynthesis process described in [2] is based on the use of a cathode modified *in situ*, whose principle has been defined and studied elsewhere [9–12]. The electrochemical reduction mechanism is established through the voltamperometric study of the NMPD reduction and the corresponding hydroxylamine (HAMPD). The modelling of the electrolysis reactor operation depends on this reaction mechanism and calculations are developed from physico-chemical data measured experimentally (rate of the hydrogen evolution reaction, viscosity, diffusion coefficients) or approximately estimated (reaction enthalpies).

The aim of the calculation is to describe the variations of the concentrations of the various species with time during a manufacturing process. The influence of operating parameters on the required duration of an operation in order to obtain a given conversion is examined; particular attention is paid to the effect of hydrodynamic conditions and to the initial quantity of nitro-alcohol. The thermal power dissipated by process irreversibilities is estimated during electrolysis.

2. Experimental details

Preparative AMPD electrolyses were performed in the galvanostatic mode in two filter-press type cells with cathodic areas of 75 and 440 cm^2, respectively. The first cell was built in the laboratory and has a 15 by 5 cm cathode. The quantity of electrolyte processed ranged between 150 and 200 cm^3. Electrolysis operations lasted between 2 and 3 h. The second reactor consisted of an Electrocell AB (Sweden) ElectroSyn Cell Module.

The cathodes were copper plates each associated with a plastic grid used as a turbulence promoter. The anodes were made of platinum plated titanium. The

anodic and cathodic compartments were separated by a cation exchange membrane (IONAC® 3470). Each electrolyte circulated in a loop consisting of a pump, a heat exchanger and a regulated temperature reservoir allowing introduction of the electrolyte or sampling. Catholyte temperature was maintained at 60° C.

During the first electrolysis operation a nitro-alcohol sulphuric aqueous solution to which a small quantity of zinc sulphate had been added was introduced into the cathodic compartment. During electrolysis the Zn^{2+} cation was reduced to a metallic zinc deposit that inhibited hydrogen reduction to the advantage of the hydroxylamine reduction. Once the amine reduction was terminated following current cut off, the electrolyte was emptied out for EED processing and it was replaced with a new quantity of nitro-derivative sulphuric solution. Prior to the start of the next operation zinc first flowed in Zn^{2+} form to precipitate once more when the cathode potential reached a value that was more negative than the Zn/Zn^{2+} equilibrium potential.

Use of a Cu–Zn cathode with a high hydrogen overvoltage did not completely inhibit the proton reduction. By operating with such a cathode and with a catholyte with an acidity ratio H^+/RX (with $RX = RNO_2 + RNHOH + RNH_2$) in the order of 1.1 it was found that hydrogen evolution began once nitro-alcohol conversion reached 67%.

Gas evolution at the cathode was measured during certain preparatory electrolyses by using a classic gas counter on an airtight cathodic circuit. The volume of hydrogen measured was brought back to normal temperature and pressure conditions following correction of the water vapour pressure.

Reaction progress was followed, during some electrolysis tests, by potentiometric analysis of the catholyte. The proportions of sulphuric acid, hydroxylamine and amine were obtained; nitro was deduced by difference. The mass balance established on the catholyte at the end of electrolysis showed up a slight loss in organic matter because of the membrane's residual permeability. Furthermore, density, viscosity and resistivity were measured, for several temperatures, on samples of catholyte taken during electrolysis.

Polarization curves were plotted on a rotating copper hemisphere ($A = 0.67\,cm^2$) in a 150 cm^3 isotherm cell using a classical three electrodes installation. Before plotting each intensity-potential curve, this electrode was polished using very fine emery cloth, then carefully rinsed with distilled water. The cathode potential was measured with respect to a saturated calomel electrode (SCE). The counter-electrode made of a platinum wire was housed in a compartment separated by sintered glass. The viscosity of the solutions was measured using an Ubbelohde viscosimeter.

3. Results and discussion

3.1. *The reaction model*

The voltamperometric curve 2 of Fig. 1 shows that the reduction on copper of a 5.87×10^{-3} M NMPD solution starts at around -0.8 V. The results of the preparative electrolyses in a sulphuric acid medium show that with $H^+/RX = 1.1$, reduction of the nitro-alcohol with 4 electrons using the massive copper electrode produces hydroxylamine [1, 2]. This reaction may be schematically described by the equation:

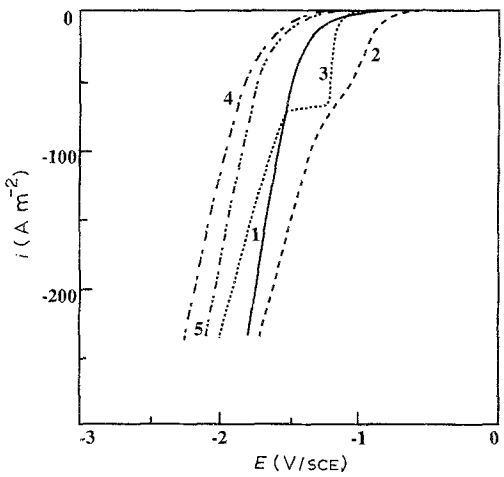

Fig. 1. Current density-potential curves on rotating electrodes. $\omega = 2000$ r.p.m.; $v = 300\,mV\,min^{-1}$; $\theta = 20°C$; [KCl] = 0.1 M. Copper hemisphere ($A = 0.67\,cm^2$): (1) ground current; (2) [NMPD] = 5.87×10^{-3} M; (3) [$ZnCl_2$] = 10.5×10^{-3} M, zinc disc ($A = 0.19\,cm^2$); (4) ground current; (5) [HAMPD] = 5.9×10^{-3} M.

First stage:

$$RNO_2 + 4H^+ + 4e^- \xrightarrow{E=-0.8\,V/SCE} RNHOH + H_2O \quad (1)$$

Solubility of the nitro-alcohols in aqueous medium may be very high: 2 to 3 mol kg^{-1} of solvent. At these concentrations the Reaction 1 is limited by the rate of charge transfer and consequently current densities higher than 3000 A m^{-2} may be applied during this phase. The concentration of RNO_2 decreased, reaching the value at which the Reaction 1 is limited by the mass transfer [13, 14] after a critical time t_{cl}. The limiting current $I_{l,l}$ is then below the imposed current I_t; there follows a decrease in electrode potential that triggers the deposit of a layer of zinc on the copper through reduction of the zinc sulphate added to the catholyte during the first operation. The cathode, thus modified *in situ*, then acquires electrocatalytic properties that favour the electrochemical reduction of the hydroxylamine and the second stage of the electrolysis begins. Curve 5 of Fig. 1 shows that the reduction of the HAMPD on the zinc or zinc-plated copper electrode starts at around -1.6 V.

2nd stage:

$$RNHOH + 2H^+ + 2e^- \xrightarrow{E=-1.6\,V/SCE} RNH_2 + H_2O \quad (2)$$

Curve 3 in Fig. 1 is relative to the reduction of the Zn^{2+} ion on the copper electrode. The metallic zinc

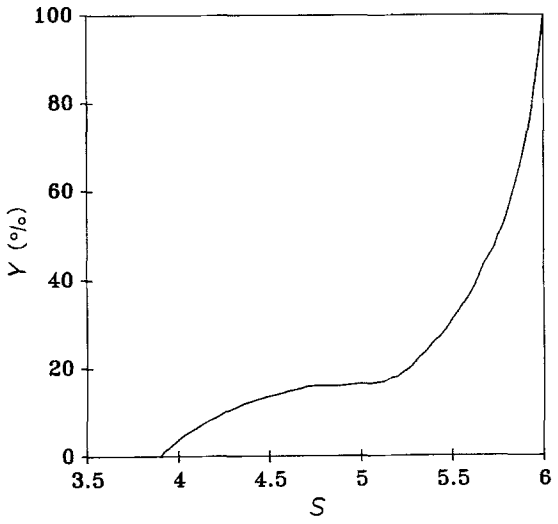

Fig. 2. Variation of the current yield for the hydrogen evolving reaction as a function of the reduction stage S of NMPD. Case of a deposit of zinc on copper during electrolysis. $C_{1,t=0} = 2400\,\text{mol m}^{-3}$; $H^+/RX = 1.1$; $\theta = 60°\,C$. Other conditions: see Table 3.

deposit on copper starts at around -1.1 V and indicates the transition between the two electrolysis stages:

$$Zn^{2+} + 2e^- \longrightarrow Zn \qquad (3)$$

During the second stage the experiment shows that hydrogen is released in significant quantities:

$$2H_2O + 2e^- \longrightarrow H_2 + 2OH^- \qquad (4)$$

Figure 2 shows the variation of the current efficiency for the co-evolution of hydrogen as a function of the reduction stage S. This current efficiency is defined by the ratio of the partial current I_4 producing H_2 to the total current I. The reduction stage S defined by Equation 11 characterizes the progress of the electrolysis.

Under certain operating conditions the concentration of hydroxylamine may reach the critical value $C_{2,tc2}$, at critical time t_{c2}, for which the Reaction 2 becomes limited by the mass transfer. As the solution becomes exhausted of hydroxylamine (end of the 2nd stage), all the zinc then remains attached to the cathode on condition current density is maintained at a sufficiently high value. Current density is controlled during electrolysis according to a clearly defined programme and its average value is about $2700\,\text{A m}^{-2}$.

During the next operation the zinc deposit is firstly dissolved in the new catholyte and then reconstitutes itself during the second phase of electrolysis and so on; between two operations the extra zinc required is very low.

It should be noted that, under the selected operating conditions, starting with the beginning of the second stage, the hydroxylamine reacts chemically on the zinc according to the global equation:

$$RNHOH + Zn + 2H^+ \longrightarrow RNH_2 + Zn^{2+} + H_2O \qquad (5)$$

Thus, the zinc deposit constitutes a cathode with a high hydrogen overvoltage and this favours Reaction 2 at the expense of hydrogen evolution (Reaction 4), during the second stage, that would otherwise be easier with the initial copper electrode [15]. Furthermore, because of the continuous cycle of Reactions 3 and 5 the zinc surface is continually renewed and this prevents any de-activation during the operation. The fraction I_3 of current due to the zinc deposit is very modest because of the low concentration of zinc sulphate ($i_3 \leqslant 120\,\text{A m}^{-2}$). Moreover, the passage of the current through the cationic membrane is due essentially to the transfer of solvated protons. The resulting transport of water leads to an increase in the volume, V, of the catholyte, which progressively reduces the amine concentration. In the case of a cationic membrane IONAC® 3470 used for laboratory cells the quantity of water migrating towards the cathodic compartment was measured to be approximately $30\,\text{g Faraday}^{-1}$. Duration of the exhaustion that terminates the second stage must thus be the shortest possible in order to favour amine concentration later on.

At the end of the electrolysis the catholyte is introduced in the EED cell made up of elements identical to those of the electrochemical reactor. This cell is equipped with an anionic membrane and the following reactions take place within the cathodic compartment:

$$(RNH_3)_2SO_4 \rightleftharpoons 2RNH_3^+ + SO_4^{2-} \qquad (6)$$

$$2RNH_3^+ \rightleftharpoons 2RNH_2 + 2H^+ \qquad (7)$$

Cathode: $$2H^+ + 2e^- \longrightarrow H_2 \qquad (8)$$

Anode: $$H_2O \longrightarrow \tfrac{1}{2}O_2 + 2H^+ + 2e^- \qquad (9)$$

In the catholyte, the sulphuric acid is separated from the amine through electrochemical reduction of the proton (Equation 8), and simultaneously by the migration of the sulphate ion through the membrane. The acid is reconstituted in the anolyte through water oxidation (Equation 9) that produces the protons necessary to balance the sulphate ion charges. The modelling study does not deal with the problem of the electro-electrodialysis.

For the two operations chemical yields are higher than 80% and current yields higher than 70% [1, 2].

3.2. *Diffusion coefficients*

The diffusion coefficients of the electroactive species were assessed using the rotating electrode method where the NMPD is concerned, and through application of semi-empirical correlations [16, 17] for the NMPD and the HAMPD.

In a sulphuric acid medium, identical to that used in preparative electrolysis, it is not possible to measure the diffusion coefficient of the RNO_2 and RNHOH reacting species even when the acid concentration is very low (10^{-2} M) because of the co-evolution of hydrogen. Consequently, the kinetic characteristics of

the electrochemical reaction (1) were determined for the case of an aqueous solution of NMPD 5.87×10^{-3} M in KCl 0.1 M.

For a reaction limited simultaneously by the charge transfer and the diffusion of the active species the current at the rotating electrode is given by [18]:

$$I^{-1} = I_k^{-1} + I_l^{-1} = I_k^{-1} + (\gamma zFACD^{2/3}\nu^{-1/6})^{-1}\omega^{-1/2} \quad (10)$$

where I_k represents the part of the current under kinetic control: $I_k = zFAk(E)C$.

The values of I_k are deduced from the graph showing I^{-1} as a function of $\omega^{-1/2}$ and from the intercept of the straight lines on the I^{-1} axis for various potential values. The slope of the Tafel line deduced from these curves is 78 mV decade^{-1}. The density of the corresponding exchange current is 3.73×10^{-3} A m^{-2}.

The NMPD diffusion coefficient is calculated from the slope of the straight lines of I^{-1} against $\omega^{-1/2}$. At 20° C, measurement of the kinetic viscosity of the solution provides: $\nu = 0.927 \times 10^{-6}$ m^2 s^{-1}. Using Equation 10 it is possible to deduce the value of the diffusion coefficient of the NMPD for these conditions: $D_1 = 3.6 \times 10^{-10}$ m^2 s^{-1} by taking $z = 4$ and $\gamma = 0.451$ rd^{-1} [19]. It was not possible to determine the HAMPD diffusion coefficient experimentally as at the potential where this species reduces on zinc (− 1.6 V) the co-evolution of hydrogen is sufficiently substantial to disturb measurement of the current on the rotating electrode, even in a neutral medium (KCl 0.1 M); no plateau was discernible for the diffusion current (*cf.* curves 4 and 5, Fig. 1). Consequently, an attempt was made to estimate this diffusion coefficient from semi-empirical correlations.

Wilke and Chang's correlation [16], applied in the case of water with an association factor $\phi = 2.6$ and an NMPD molar volume: $V_{m,1} = 0.1401$ m^3 kmol^{-1} [20], leads to a value $D_1 = 8.2 \times 10^{-10}$ m^2 s^{-1}, very close to that provided by Lusis and Ratcliff's correlation [17]: $D_1 = 7.8 \times 10^{-10}$ m^2 s^{-1}. Values of D_1 measured and calculated for the same viscosity only agree as to size. However, in the absence of any experimental data on the HAMPD we used Wilke and Chang's correlation to estimate its coefficient D_2 by using as a molar volume the value: $V_{m,2} = 0.1363$ m^3 kmol^{-1}. The value found is slightly higher than D_1: $D_2 = 8.4 \times 10^{-10}$ m^2 s^{-2}.

Table 1. Experimental values of volumic mass and kinematic viscosity of the catholyte for different values of the reduction stage of the sulphuric aqueous solution of NMPD. Initial NMPD molality = 2.92 mol kg^{-1}; $H^+/RX = 1.1$

Reduction stage (S)	*Volumic mass (kg m^{-3})*		*Kinematic viscosity $10^6\nu$ (m^2 s^{-1})*	
	θ = 45° C	*θ = 60° C*	*θ = 45° C*	*θ = 60° C*
0.00	1225	1215	2.724	1.888
1.07	1191	1180	2.181	1.530
2.87	1166	1156	2.135	1.540
6.00	1097	1089	1.393	1.031

Calculations of electrolysis simulation were performed using Wilke and Chang's equation to calculate mass transfer coefficients. The kinematic viscosities used in these calculations are given in Table 1.

4. Representing the model

The calculation technique is based on the reaction mechanism described previously. It enables simulation of an electrolysis operation performed in galvanostatic mode (I, constant current), or otherwise in the galvanostatic regime with intensity programmed in time ($I = f(t)$) as is the case with electrolyses performed in the two cells with cathodic areas equal to 0.044 and 1.6 m^2, respectively. The model makes it possible to foresee variations in RX compound concentrations with time. It is practical to define a parameter called the reduction stage in order to characterize the reaction progress:

$$S_t = V_t[z_1 C_{2,t} + (z_1 + z_2)C_{4,t}]/n_{1,t=0} \quad (11)$$

where S, V, C_2 and C_4 vary as functions of time t. $z_1 = 4$ and $(z_1 + z_2) = 6$ are the total electron numbers transferred for Reactions 1 and 1 + 2, respectively. The term $n_{1,t=0}$ represents the initial amount of NMPD dissolved in the initial catholyte volume $V_{t=0}$. $C_{2,t}$ and $C_{4,t}$ are the concentrations of NMPD and AMPD at time t.

The installation includes a recycling tank containing a volume V_t of catholyte that is assumed to be large with relation to the volume of the cell. Furthermore, it is assumed that flow within the filter-press reactor is of piston type. The known models [13, 21] describing the temporal variation of an electroactive species in this type of installation were developed on the assumption that the electrolyte volume does not vary. In the present case, because of the importance of the increase of the catholyte volume with time, RX species concentrations were calculated by assuming that V_t increases by an increment ΔV between the successive time intervals Δt.

This increment ΔV was calculated using the measurement of the increase in catholyte volume in the laboratory cell, operating with the same solutions and the IONAC® 3470 membrane. Calculations were as follows:

$$\Delta V = Q_t \Delta v/F \quad \text{with } \Delta v = 30\,\text{cm}^3\,\text{Faraday}^{-1} \quad (12)$$

with

$$Q_t = \int_0^t I_t \mathrm{d}t \quad (13)$$

4.1. *Calculations for the first stage*

Q_t is calculated as follows:

$$Q_t = \sum_{t=0}^{t} I_t \Delta t = \sum_{t=0}^{t} \Delta Q_{1,t} = Q_{1,t} \quad (14)$$

The Δt calculation step is selected as very small with respect to the duration of the electrolysis. The calculations during this first electrolysis phase are done

assuming that the current efficiency for Reaction 1 is 100%. In fact, in some experiments the analyses reveal the formation of a slight amount of amine a little before the maximum of the RNHOH concentration (Fig. 4). But in the absence of a kinetic law for the formation of amine in the first stage, it is assumed that only the Reaction 1 takes place on the cathode as long as the limiting current $I_{1,1}$ for RNO_2 reduction, calculated by means of Equation 19, remains higher than the operating intensity I_t; the current relative to the Reaction 1 is then limited by the charge transfer (the value of $C_{1,t}$ is high). The variation in the number of RNO_2 moles is provided by

$$n_{1,t=0} - n_{1,t} = Q_t/(z_1F) \quad (15)$$

The concentrations $C_{1,t}$ of RNO_2 and $C_{2,t}$ of RNHOH at time t are deduced:

$$C_{1,t} = n_{1,t}/V_t \quad (16)$$

$$C_{2,t} = (n_{1,t=0} - n_{1,t})/V_t \quad (17)$$

with

$$V_t = V_{t=0} + \sum_{t=0}^{t} \Delta V \quad (18)$$

When the concentration $C_{1,t}$ of RNO_2 has decreased sufficiently, its reduction rate then becomes limited by mass transfer. The RNO_2 reduction limiting current, calculated using the equation [13]:

$$I_{i,1} = z_iFNC_{i,t}M_i \quad (19)$$

(with $i = 1$) is compared, for each step of the calculation, with the operating current I_t. When the concentration $C_{1,t}$ of RNO_2 reaches a value such that $I_{1,1} \leqslant I_t$ (with critical time t_{cl}; *cf.* Figs 3 and 5) it is assumed that the zinc electrodeposition, and the second stage both begin simultaneously. From the critical time t_{cl} the concentration $C_{1,t}$ of RNO_2 decreases exponentially with time and may be calculated for an interval Δt using the following equation ($i = 1$):

$$C_{i,t} = C_{i,(t-\Delta t)} \exp(-\Delta t M_i/\tau_t) \quad (20)$$

The Δt calculation step for the first stage is chosen by determining an approximate value t'_{cl} of the critical time relative to the Reaction 1. This value is calculated by assuming that the catholyte volume remains constant and equal to the initial volume $V_{t=0}$ and that the current also remains constant:

$$t'_{cl} = (z_1FV_{t=0}C_{1,t=0}/I) - \tau_{t=0}/M_1 \quad (21)$$

The value chosen for Δt is a small fraction of t'_{cl} ($\Delta t = t'_{cl}/200$ for example); the volume of catholyte is then calculated for each step using Equation 18. The mass transfer coefficient k_i used to calculate the term M_i is given by Carlsson [22]:

$$k_i = 5.57(D_i/De)Re^{2/5}Sc^{1/3} \quad (22)$$

for the ElectroSyn cell.

4.2. *Calculations for the second stage*

For an electrode reaction whose rate is limited by the mass transfer (case of Reaction 1 during stage 2, and of Reaction 2 at the end of stage 2), the decrease of the concentration of the reactive species i is exponential in the Δt interval (Equation 20 with $i = 1$ and 2).

The quantities of electricity in Reactions 2 and 3 during the second stage, and in Reaction 2 at the end of the second stage, are calculated by integrating the currents $I_{i,1}$ as a function of t for each Δt interval, that is:

$$\Delta Q_{i,t} = z_iFNC_{i,(t-\Delta t)}\tau_t[1 - \exp(-\Delta t M_i/\tau_t)] \quad (23)$$

The experiment shows that hydrogen evolution occurs at the beginning of the second stage. During this phase the current I_2 concerned with Reaction 2 is provided by:

$$I_{2,t} = I_t - (I_{1,1} + I_{3,1} + I_{4,t}) \quad (24)$$

in which $I_{1,1}$ and $I_{3,1}$ are calculated by Equation 19. In the computations it is assumed that the rate of Reaction 5 may be neglected compared to that of Reaction 3, therefore the deposition current I_3 is taken equal to the limiting current as soon as the critical time t_{cl} is reached. The current $I_{4,t}$ is provided by a correlation that is experimental in origin, as a function of the reduction stage S_t (*cf.* Fig. 2):

$$I_{4,t} = 0.01I_t(8703.26 - 7923.22S_t + 2677.34S_t^2 - 398.24S_t^3 + 22.04S_t^4) \quad (25)$$

The concentration $C_{2,t}$ of RNHOH during the second phase is calculated from the total quantity of electricity:

$$C_{2,t} = [C_{2,tcl}V_{tcl} + \sum_{t_{cl}}^{t} \Delta Q_{1,t}/(z_1F) - Q_{2,t}/(z_2F)]/V_t \quad (26)$$

where $C_{2,tcl}V_{tcl}$ represents the number of RNHOH moles formed at the critical instant t_{cl}; $\Sigma_{t_{cl}}^{t} \Delta Q_{1,t}$ is the quantity of electricity used since t_{cl} for Reaction 1; and with

$$Q_{2,t} = Q_t - \sum_{t_{cl}}^{t} \Delta Q_{1,t} - \sum_{t_{cl}}^{t} \Delta Q_{3,t} - \sum_{t_{H2}}^{t} \Delta Q_{4,t} \quad (27)$$

where $\Sigma_{t_{cl}}^{t} \Delta Q_{3,t}$ and $\Sigma_{t_{H2}}^{t} \Delta Q_{4,t}$ are the quantities of electricity used respectively for Reactions 3 and 4 and t_{H2} represents the instant when hydrogen evolution begins.

The amine concentration is deduced from

$$C_{4,t} = Q_{2,t}/(z_2FV_t) \quad (28)$$

At the critical time t_{c2}, the concentration of RNHOH had sufficiently diminished for condition $I_{2,1} \leqslant I_2$ to be satisfied. This instant marks the start of the period where the hydroxylamine is exhausted; its concentration then varies as an exponential function of the time during each Δt interval (*cf.* Equation 20 for $i = 2$).

Accumulated current yield is calculated from the start of the hydrogen evolution ($S = 3.9$) by the equation

$$R = (Q_{1,t} + Q_{2,t})/Q_t \quad (29)$$

and instantaneous current yield is provided by

$$R_t = (I_{1,t} + I_{2,t})/I_t \quad (30)$$

In practice, the electrolysis is considered to be terminated once $S \geqslant 5.95$.

4.3. *Calculation of thermal effects*

Electrochemical reactions performed at finite rates lead to irreversibilities linked on the one hand to ionic transport phenomena through the electrolytes and the separator, and on the other hand, to overvoltage at the electrodes. These irreversibilities become apparent as heat is released. This heat release should be determined in order to calculate the area of the necessary heat exchangers. The thermal energy P_{th} to be extracted at each instant is the difference between the total electric power UI consumed at the cell terminals and the enthalpy of the chemical transformations caused by the passage of the current:

$$P_{th} = P_{elec} - \Sigma \dot{n}_i \Delta H_i \quad (31)$$

where $\dot{n}_i$ is the rate of the ith reaction:

$$\dot{n}_i = I_i/(z_i FA) \quad (32)$$

The chemical reactions taken into account are the cathodic Reactions 1, 2 and 4 each associated with the anode Reaction 9. Reaction 3 is not taken into account because of the very low value of the current I_3. ΔH_i enthalpies of the global reactions:

$$RNO_2 + H_2O \longrightarrow RNHOH + O_2 \quad (1')$$

$$RNHOH \longrightarrow RNH_2 + \tfrac{1}{2}O_2 \quad (2')$$

were evaluated using combustion enthalpies of compounds of the same family (nitropropane, propylamine) assuming that the thermal effects relative to the two successive stages (Reactions 1′ and 2′) are within the same ratio for nitrobenzene and its derivatives on the one hand, and NMPD and its derivatives, on the other hand (*cf.* Table 2). In these calculations mixture and protonation enthalpies are not taken into account.

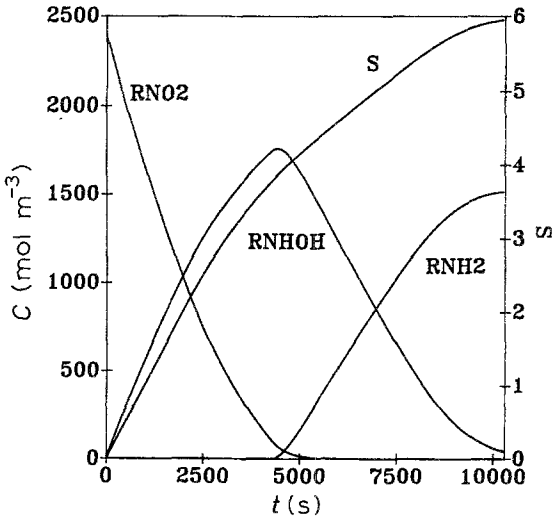

Fig. 3. Calculated variations of the HAMPD and AMPD concentrations and of the reduction stage as functions of time during electrolysis of an NMPD solution. Cathode: initially copper; after t_{cl}: zinc on copper. ElectroSyn Cell with a cathode of 0.044 m^2 (see Table 3). $C_{1,t=0} = 2400\,mol\,m^{-3}$; $H^+/RX = 1.1$; $N = 1000\,dm^3\,h^{-1}$; $V/A = 0.017\,m$; $V = 0.75\,dm^3$; $t_{cl} = 4280\,s$; for $t = t_{cl}$: $S = 3.78$.

5. Discussion

The geometrical characteristics of the ElectroSyn Cell (Electrocell AB) for which calculations were made, together with some of the operating conditions are summed up in Table 3. The calculation technique can be easily adapted to the ElectroprodCell with a cathodic area of 1.6 m^2.

Figure 3 shows the variation in concentrations of the various species calculated during a current programming time such as the values of the initial and terminal current density were respectively 4000 and 2000 A m^{-2} (*cf.* Table 3), and for an initial concentration of NMPD equal to 2400 mol m^{-3}. The critical time t_{cl} was 4280 s which corresponds to the condition $I_{1,1} = I$ at which the zinc electrocrystallization occurs (*cf.* Fig. 5). This instant also corresponds to the maximum HAMPD concentration (1760 mol m^{-3}). For a reduction stage of 5.95 the concentration of NMPD

Table 2. Reaction enthalpy (kJ mol^{-1}) for Reactions (1′), (2′) and (4) + (9). Data from combustion enthalpy [23]

$CH_3CH_2CH_2NO_2(liq) + H_2O(liq) \longrightarrow CH_3CH_2CH_2NH_2(liq) + \frac{3}{2}O_2$	$\Delta H(a) = 364.91$
$C_6H_5NO_2(liq) + H_2O(liq) \longrightarrow C_6H_5NH_2(liq) + \frac{3}{2}O_2$	$\Delta H(b) = 303.05$
$C_6H_5NO_2(liq) + H_2O(liq) \longrightarrow C_6H_5NHOH(liq) + O_2$	$\Delta H(b, 1) = 269.6$ $\Delta H(b, 1) = 0.89*\Delta H(b)$
$C_6H_5NHOH(liq) \longrightarrow C_6H_5NH_2(liq) + \frac{1}{2}O_2$	$\Delta H(b, 2) = 33.44$ $\Delta H(b, 2) = 0.11*\Delta H(b)$
$NMPD + H_2O \longrightarrow HAMPD + O_2$	$\Delta H(1') = 0.89*\Delta H(a)$ $\Delta H(1') = 325$
$HAMPD \longrightarrow AMPD + \frac{1}{2}O_2$	$\Delta H(2') = 0.11*\Delta H(a)$ $\Delta H(2') = 40$
$H_2 + \frac{1}{2}O_2 \longrightarrow H_2O$	$\Delta H(4) + (9) = 285.6$

Table 3. Electrochemical reduction of nitro-alcohols. Characteristics of the ElectroSyn Cell (cathode area: 0.044 m^2), and parameters used for the preparation of AMPD under galvanostatic conditions

Parameter	*Symbol*	*Value*	*Unit*
Electrode width	b	0.148	m
Electrode length	l	0.297	m
Cathode-membrane distance	h	0.009	m
Volumic flow	N	(8.33–41.7) × 10^{-5}	$m^3 s^{-1}$
Linear fluid velocity	v	(6.26–31.3) × 10^{-2}	$m s^{-1}$
Mass transfer coefficients	k_1, k_2	(4.5–8.6) × 10^{-5}	$m s^{-1}$
Initial concentration of RNO_2	$C_{1,t=0}$	800–2400	$mol m^{-3}$
Initial current density	$i_{t=0}$	4000	$A m^{-2}$
Final current density	i_f	2000	$A m^{-2}$
Cell voltage	U	3.5–5.4	V
Temperature	θ	60	°C

An example of current density and voltage variations used in the present computations:
$S < 2$: $i\,(A m^{-2}) = i_{t=0}$; $S > 4$: $i = i_f$; $2 < S < 4$: $i = 3i_f - 0.5 i_f S$
$S < 2.8$: $U(V) = 3.5 + 0.458S$; $S > 5.4$: $U = 4.8 + (S - 5.4)$

remaining is then less than 10^{-4} mol m^{-3}, that of HAMPD has dropped to 4.17 mol m^{-3}, whereas the concentration of AMPD is of 1520 mol m^{-3}. This value, noticeably lower than the initial concentration of RNO_2, is due to dilution of the catholyte. The accumulated current yield is 87%, and the instantaneous current yield is only 16% because of the high level of hydrogen evolution in contrast with the low concentration of hydroxylamine. The HAMPD partial reduction current is still 14 A for a total current of 88 A.

Figure 4 shown in dimensionless coordinates presents the comparison of the calculation results with those of an experiment where NMPD, HAMPD and AMPD concentrations were followed by potentiometric analysis. The concentration variation curves agree rather well. Discrepancies in the concentration variation curves of the reagent and the products may in part be attributed to the inaccuracy of the method for determining the equivalent point for these compounds. The highest discrepancy between the model and the experiment where AMPD was concerned lies between the values 2.5 and 4 in the reduction stage. Indeed, the model only takes hydroxylamine reduction into account from the moment where the theoretical conditions for the zinc electrodeposition were achieved (S = 3.8 in the case of Fig. 4), whereas the analysis proves its appearance at around S = 2.5. However, the discrepancy between forecast and the experiment is relatively low in the interval: $3 < S < 4.2$ because of the slow rate of amine formation on copper for these conditions; it only shows itself as a difference in concentration of the order of 5 to 7% on the maximum hydroxylamine concentration. A more complicated model, requiring more numerous kinetic data and a calculation mode based on a voltage balance, is not necessary for fulfilling the objective of a forecast study of the behaviour of a pilot scale installation.

Figure 5 shows variations of partial currents with time for Reactions 1 to 4 and of the total current, the

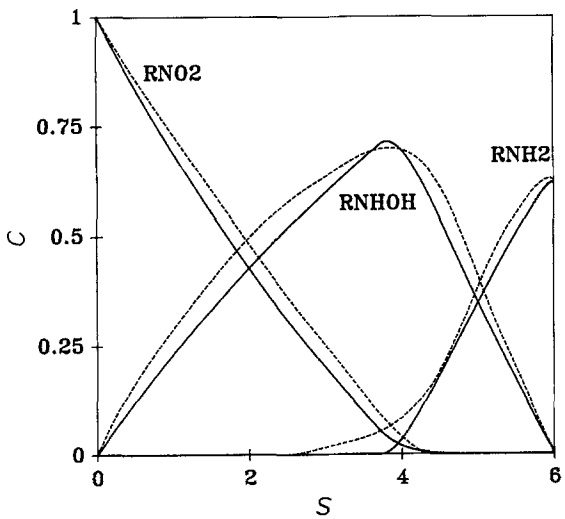

Fig. 4. Calculated (full lines) and experimental (dashed lines) values of the dimensionless concentrations of NMPD, HAMPD and AMPD as functions of the reduction stage. ElectroSyn Cell (see Table 3). AMPD starts to appear at S = 2.4. Calculations for: S_f = 5.99; N = 500 $dm^3 h^{-1}$; V/A = 0.0144 m.

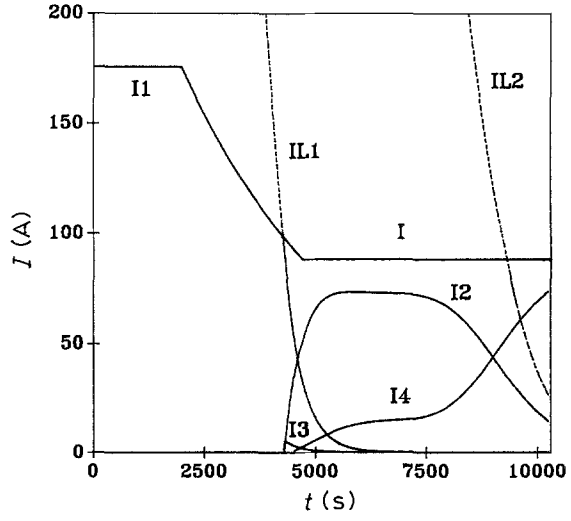

Fig. 5. Variations of the partial currents calculated for the electrolysis of a NMPD solution under galvanostatic conditions. ElectroSyn Cell (see Table 3). $C_{1,t=0}$ = 2400 mol m^{-3}; H^+/RX = 1.1; N = 1000 $dm^3 h^{-1}$; V/A = 0.017 m; Calculated: t_{el} = 4280 s; $I_{1,2} > I_2$ for S = 5.95. $I_{1,1}$ and $I_{1,2}$ are the diffusion limiting currents for NMPD and AMPD. Reduction of NMPD: I_1; HMPD: I_2; Zn^{2+}: I_3; hydrogen evolution: I_4. Total current: I ($I = I_1$ for $t < t_{el}$).

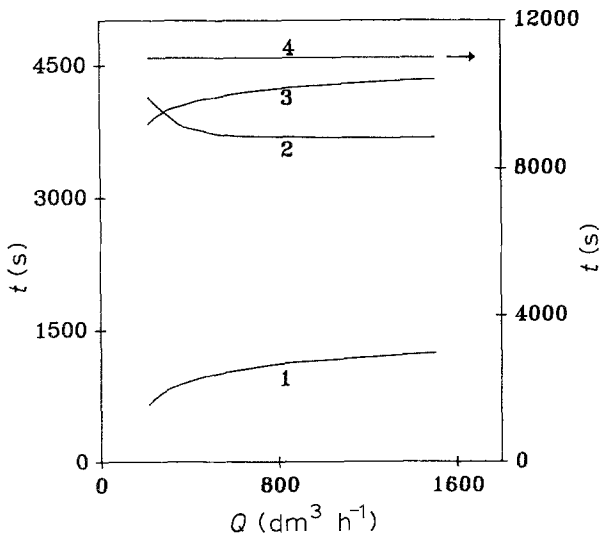

Fig. 6. Calculated values of the critical time t_{cl} and of the total duratin t_f of the electrolysis as functions of the volumic flow rate N to reach $S = 5.99$ in the case of an NMPD solution. $C_{1,t=0} = 800\,mol\,m^{-3}$: (1) t_{cl}; (2) t_f. $C_{1,t=0} = 2400\,mol\,m^{-3}$: (3) t_{cl}; (4) t_f. ElectroSyn Cell with a $0.044\,m^2$ cathode; $V/A = 0.017\,m$; for other conditions see Table 3.

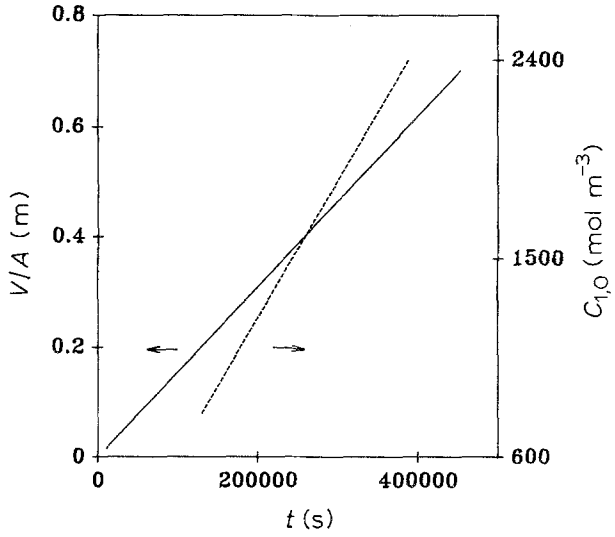

Fig. 8. Calculated electrolysis duration as a function of the initial quantity of solution (NMPD: $C_{1,t=0} = 2400\,mol\,m^{-3}$), and as a function of the initial NMPD concentration $C_{1,t=0}$. ElectroSyn Cell ($A = 0.044\,m^2$) and industrial conditions of AMPD production: $V/A = 0.6\,m$. $N = 1000\,dm^3\,h^{-1}$; $S = 5.99$; for other conditions see Table 3.

current I_4 being calculated by the correlation using Equation 25. The instantaneous values of the reduction limiting currents for RNO_2 ($I_{1,1}$) and RNHOH ($I_{2,1}$) are also shown. Figure 5 represents the results of the calculation corresponding to typical conditions for a preparative electrolysis. At the beginning of electrolysis the current I_1 is identical with the total current I (100% current yield), then when the curves respectively providing I and $I_{1,1}$ meet again, the values of the intensities I_1 and $I_{1,1}$ are equal again. However, for the planned conditions, the $I_{2,1}$ current does not meet with the I_2 current, and in consequence, the limitation through mass transfer does not have an influence on electrolysis duration (*cf.* curve 4, Fig. 6); this result matches the experimental observations.

The influence of the mass transfer on the duration of the electrolysis is sensitive when catholyte flow is less than $800\,dm^3\,h^{-1}$ ($v < 0.17\,m\,s^{-1}$; $k_2 < 7.3 \times 10^{-5}\,m\,s^{-1}$) as shown by curve 2 of Fig. 6 in the case of a low initial concentration of NMPD. This extension of the duration of the electrolysis is the result of the fall in the mass transfer coefficient (k_2 varies from 8.6×10^{-5} to $4.5 \times 10^{-5}\,m\,s^{-1}$ when N falls from $1500\,dm^3\,h^{-1}$ to $300\,dm^3\,h^{-1}$). In accordance with Equation 21 critical time t_{cl} increases as a function of flow (curves 1 and 3 of Fig. 6).

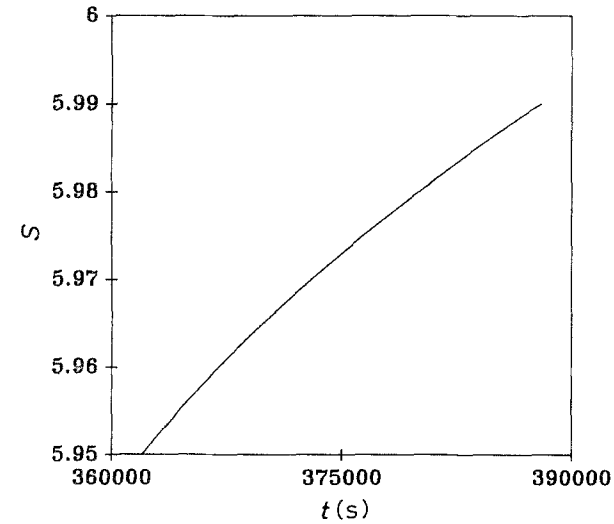

Fig. 7. Calculated values of the electrolysis duration of an NMPD solution ($C_{1,t=0} = 2400\,mol\,m^{-3}$) against the reduction stage S under industrial conditions for AMPD production. $V/A = 0.6\,m$; $N = 400$ to $1000\,dm^3\,h^{-1}$; for other conditions see Table 3.

Electrolysis duration is sensitive to the required reduction stage as shown in Fig. 7 for conditions close to those planned for industrial electrolysis. The increase of conversion takes place at the cost of a slight drop in accumulated current yield, for example it drops from 87 to 83%, when the conversion increases from 5.95 to 5.99. This improvement of conversion implies an increase in the duration of electrolysis of about 7% (*cf.* Fig. 7) for an AMPD dilution effect of less than 1%.

The duration of the electrolysis also depends on the initial quantity of NMPD to reduce. With the aim of discontinuous mode manufacture, on an industrial scale, it is important to know the initial volume $V_{t=0}$ of solution to electrolyse over a period of 4 days for an installation whose cathodic area is A. Figure 8 shows the variation of the operating duration to reach a reduction stage of 5.99 with standard operating conditions ($C_{1,t=0} = 2400\,mol\,m^{-3}$; $N = 1000\,dm^3\,h^{-1}$). This curve allows prediction of the quantity of NMPD likely to be processed in 96 h up to the reduction stage where $S = 5.99$ is 173 kg (1285 mol) per m^2 of cathodic area of an ElectroSyn Cell type. It may be contained in an initial catholyte volume of $0.535\,m^3$. In order to reach this reduction stage electrolysis leads to a relatively high increase in catholyte volume as the final volume calculated is $0.824\,m^3$. The final concentration of AMPD is then $1540\,mol\,m^{-3}$.

The curve showing the variation in the thermal

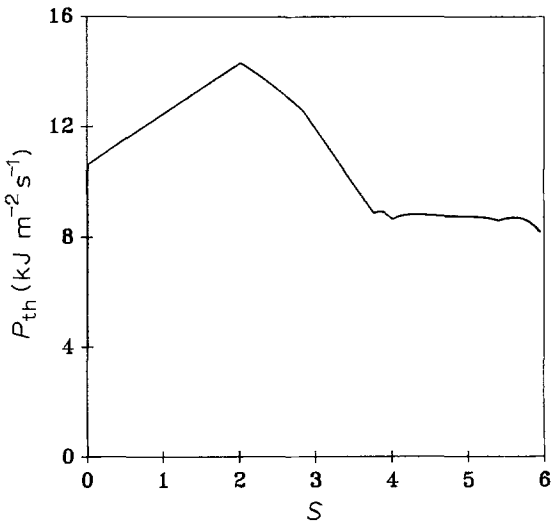

Fig. 9. Variation of the thermal power dissipated as a function of the reduction stage S. Case of the ElectroSyn Cell: see Tables 2 and 3 for the calculation conditions. NMPD: H^+/RX = 1.1; $C_{1,t=0}$ = 2400 mol m^{-3}.

energy, P_{th}, to be removed in order to maintain the system at a constant temperature as a function of the transformation progress is shown in Fig. 9. The maximum is situated at around S = 2; its value is in the order of 14.3 kW m^{-2} of cathodic area. The initial increase in the thermal energy mainly results from the increase in voltage at the terminals due to the increase in the resistivity of the catholyte resulting from reduction of the AMPD (*cf.* Table 4). Indeed, the initial reagent of molecular nature, is then replaced by the HAMPD that captures sulphuric acid free protons to provide the corresponding hydroxylammonium ion which has very low mobility when compared to that of the H^+. Up to S = 2, the kinetic viscosity of the solution falls by 44% (Table 1), but the decrease in conductivity (*cf.* Table 4) through substitution of H^+ by RNH_2OH^+ has a dominant effect. The thermal energy becomes stable with values of S higher than 4 because of the relative stabilization of the resistivity; indeed, the RNH_2OH^+ and RNH_3^+ species have mobilities of a similar order.

6. Conclusion

Using voltamperometric techniques has made it possible to describe the operating mechanism for a copper cathode modified *in situ* by an electrochemical zinc deposit. At the beginning of the electrolysis the nitroalcohol can be easily reduced on copper, and once its concentration has decreased sufficiently the polarization acquired in galvanostatic mode by the cathode triggers the modification of its electrocatalytic activity by the formation of a layer of zinc that lowers the hydrogen evolution potential. An initial very low concentration of zinc salt is sufficient to induce this profound change in the cathode activity and, furthermore, this element can be fully recovered at the beginning of the next operation.

Definition of the series of reaction stages led to a simple model making it possible to simulate the electrolysis process in discontinuous mode in the practical case of a filter-press reactor coupled to a recycling tank. The model, satisfactorily tested through operation of a small pilot installation (A = 0.044 m^2), confirmed the absence of mass transfer limitation during a manufacturing process performed under commercial operating conditions.

The model is a useful aid in estimating the influence of any modification to the time scale with relation to the variation of the ratio of the quantity of reagent to the area of the electrode used.

Table 4. Values of the conductivity of the catholyte for different reduction stages of NMPD in H_2SO_4 aqueous solution. Initial NMPD molality: 2 mol kg^{-1}; H^+/RX = 1.1

Reduction stage	*Resistivity: $\rho \times 10^2$ (Ω m)*		
	θ = 30° C	*θ = 50° C*	*θ = 80° C*
0.00	3.65	2.90	2.50
0.58	4.25	3.40	2.90
3.74	16.1	12.5	9.60
4.22	17.9	13.2	9.70
4.50	18.2	13.5	9.90
5.50	16.3	12.1	8.85
6.00	15.7	11.5	8.45

Acknowledgements

The authors would like to thank Electricité de France for providing a part of the equipment used in this work.

References

[1] French Patent 2 577 242.
[2] French Patent 2 614 044.
[3] M. M. Baizer and H. Lund, 'Organic Electrochemistry', 2nd ed., Marcel Dekker, New York (1985).
[4] N. L. Weinberg and B. V. Tilak, 'Technique of Electroorganic Synthesis', Part III, John Wiley & Sons, New York (1982).
[5] A. Cyr, P. Huot, J. F. Marcoux, G. Belot, E. Laviron and J. Lessard, *Electrochim. Acta* **34** (1989) 439.
[6] US Patent 2 485 982.
[7] A. Savall, M. Rignon, G. Le Nard and J. Malafosse, Proceed., 2ème Congrès Français de Génie des Procédés, Toulouse, 5–7 September 1989.
[8] A. Savall, M. Rignon and J. Malafosse, Proceed. Joint Meeting of DECHEMA and the Society of Chemical Industry, 'Electrochemical Cell Design and Optimization Procedures', Bad Soden FRA, 24 September 1990.
[9] A. Savall, M. Giron, F. Lapicque, L. Weise and A. Storck, *Bull. Soc. Chim.* (1985) 1056.
[10] K. K. Yagii and K. K. Oshio, US Patent 4 162 948 (1979).
[11] G. Ellaly, Thèse 3ème Cycle, Université Paul Sabatier, Toulouse (1980).
[12] A. Savall, R. Abdelhedi, S. Dalbéra and M. L. Bouguerra, *Electrochim. Acta* **35** (1990) 1727.
[13] F. Cœuret, A. Storck, Eléments de Génie Electrochimique, Lavoisier, Paris (1984).
[14] M. L. Hitchman, J. P. Millington, T. R. Ralph and F. C. Walsh, *I. Chem. E. Symp. Series* **112** (1989) 223.
[15] S. Trasatti, *J. Electroanal. Chem.* **39** (1972) 163.
[16] C. R. Wilke and P. Chang, *A.I.Ch.E. J.* **1** (1955) 264.
[17] M. A. Lusis and G. A. Ratcliff, *Can. J. Chem. Eng.* **46** (1968) 385.
[18] V. G. Levich, 'Physicochemical Hydrodynamics', Prentice-Hall, Englewood Cliffs, NJ (1962) pp. 60–72.
[19] J. Newman, *J. Electrochem. Soc.* **119** (1972) 69.

[20] P. E. Liley and W. R. Gambill, Physical and Chemical Data, 'Chemical Engineer's Handbook', 5th ed. (edited by R. H. Perry and C. H. Chilton), McGraw-Hill, New York (1973) chap. 3.
[21] D. J. Pickett, 'Electrochemical Reactor Design', Elsevier, London (1977).
[22] L. Carlsson, B. Sandegren and D. Simonsson, *J. Electrochem. Soc.* **130** (1983) 342.
[23] R. C. Weast, 'Handbook of Chemistry and Physics', 64th ed., CRC Press, (1983).